Photodissociation of Bromoform at 248 nm: Single and Multiphoton Processes

Peng Zou,[†] Jinian Shu,[‡] Trevor J. Sears,[§] Gregory E. Hall,[§] and Simon W. North*[,†]

Chemistry Department, Texas A&M University, P.O. Box 30012, College Station, Texas 77842, Chemical Sciences Division, Lawrence Berkeley Laboratory, University of California, and Chemistry Department, University of California, Berkeley, California 94720, and Chemistry Department, Brookhaven National Laboratory, Upton, New York 11973-5000

Received: August 29, 2003; In Final Form: December 10, 2003

We have performed photodissociation experiments on $CHBr_3$ at 248 nm using VUV ionization photofragment translational spectroscopy. Prompt C−Br bond fission is the dominant single-photon dissociation channel. In addition to primary Br and $CHBr_2$ signals, we observe Br, CHBr, CBr, HBr, and Br_2 products attributed to secondary photodissociation of $CHBr_2$ and CHBr. There are three competing fragmentation channels from the photodissociation of $CHBr_2$: CHBr + Br, CH + Br_2, and CBr + HBr. The conclusion that Br_2 fragments do not arise from a single-photon channel in appreciable yield is supported by transient FM absorption measurements of the CHBr radical. Because the molecular HBr and Br_2 detachment channels are multiphoton processes, they will have very little impact on the atmospheric chemistry of $CHBr_3$. We conclude that the most important photodissociation channel of $CHBr_3$ in the UV region is C−Br bond breaking.

I. Introduction

The role of anthropogenic chlorine and bromine containing molecules in stratospheric ozone depletion has been well established.[1] The importance of bromine and its chemistry on the atmosphere is receiving renewed interest on the basis of predictions that bromine is almost 100 times more destructive to stratospheric ozone than chlorine on an atom for atom basis.[2,3] The role of bromoform ($CHBr_3$) as a dominant source of stratospheric bromine, however, has been the subject of recent debate.[3] The absorption spectrum of bromoform is significantly red-shifted compared to the spectra of other organic bromine compounds.[4] Theoretical calculations indicate that triplet excited states of bromoform may contribute to the absorption at wavelengths longer than 300 nm.[5] The excitations to the first several low-lying excited singlet and triplet states primarily arise from the promotion of an electron from the Br nonbonding orbital to the antibonding C−Br σ^* orbital. Therefore, the photodissociation of bromoform in the UV region is expected to result in simple C−Br bond fission. A photofragment translational spectroscopy (PTS) experiment at 193 nm with VUV ionization detection by McGivern et al. concluded that the C−Br bond cleavage was the only primary dissociation channel.[6] The $CHBr_2$ photofragments were produced with sufficient internal energy to undergo secondary dissociation, producing both CHBr + Br and CBr + HBr with quantum yields of 0.3 and 0.4, respectively. The result was a total Br atom quantum yield of 1.5 ± 0.2. Recently, Sander and co-workers performed Br quantum yield measurements from 266 to 344 nm using atomic resonance fluorescence detection.[7] Their results suggest that Br quantum yields from bromoform photodissociation at wavelengths greater than 300 nm are unity, which is consistent with theoretical prediction. However, the measured Br quantum yield at 266 nm was 0.76 ± 0.03, suggesting the existence of alternative dissociation pathways or radiationless processes. The latter, in particular, will significantly affect the atmospheric modeling of this compound. The UV photodissociation experiments of bromoform at 234 and 267 nm by Xu et al. using velocity map ion-imaging suggest nonunity Br quantum yields at both wavelengths. The authors reported that the Br_2 elimination channel is an important primary single-photon dissociation channel at the wavelengths studied with quantum yields of 0.2−0.3.[8]

Any investigation of single-photon chemistry, however, must account for the role of multiphoton dissociation channels in the interpretation of experimental results. The multiphoton dissociation of the $CHBr_3$ has proven a convenient means to produce CH($X^2\Pi$) radicals with high yield.[9−13] Lichtin et al. observed CH($A^2\Delta \rightarrow X^2\Pi$) and CH($B^2\Sigma^- \rightarrow X^2\Pi$) emission spectra in their photodissociation experiment of bromoform at 266 nm.[14] Several possible reaction pathways have been proposed for the multiphoton processes, which involve either CHBr or $CHBr_2$ as intermediates. The CH emission from the multiphoton dissociation of bromoform at 193 and 248 nm has also been studied by Lindner et al.[15] The rovibrational state distribution of CH($A^2\Delta$) fragment was measured by using time-resolved Fourier transform emission spectroscopy. The power dependence of the CH($A^2\Delta \rightarrow X^2\Pi$) fluorescence was second order and third order at 193 and 248 nm, respectively. Although a sequential fragmentation mechanism was developed to rationalize their two-laser molecular beam experiment results, the identity of the intermediates could not be definitively determined.

The CHBr fragment has been studied by Sears and co-workers[16,17] and Liu et al.[18] using the photodissociation of bromoform and transient frequency modulation spectroscopy. Recently, Liu et al. proposed that nascent CHBr radicals from photodissociation of bromoform at 266 nm were significantly more energetic than those produced at 193 nm on the basis of the measured appearance kinetics. The result suggests that the CHBr fragments at 266 nm may arise from a multiphoton process because the energetics of CHBr formation via one

* Corresponding author. E-mail: swnorth@tamu.edu.
[†] Texas A&M University.
[‡] University of California.
[§] Brookhaven National Laboratory.

10.1021/jp0310394 CCC: $27.50
Published on Web 02/10/2004

photon at 193 nm, due to spontaneous secondary dissociation of $CHBr_2$, and via primary Br_2 elimination at 266 nm should be similar.

Despite all this previous work on UV photodissociation of bromoform, key questions remain unsettled. What are the primary dissociation channels? How do the branching ratios depend on excitation wavelength? What is the role of multiphoton processes? We have studied the photodissociation of $CHBr_3$ at 248 nm using photofragment translational spectroscopy (PTS) with VUV ionization detection. The power dependence and forward convolution fitting of the time-of-flight mass spectra reveal that the dominant primary dissociation channel is $CHBr_2 + Br$. We find that the molecular bromine product arises from the secondary photodissociation of the resulting $CHBr_2$ radicals, in competition with Br and HBr elimination.

II. Experiment

The experiments were carried out at the Chemical Dynamics Beamline at the Advanced Light Source (ALS) of Lawrence Berkeley National Laboratory. A complete description of the rotating-source fixed-detector apparatus can be found elsewhere.[19] Briefly, a pulsed molecular beam of <1% $CHBr_3$ seeded in helium was collimated with conical skimmers and intersected at 90° with the output of an excimer laser operating on the KrF transition (248 nm). Neutral photodissociation products traveled 15.1 cm, where they were ionized by tunable VUV undulator radiation, mass selected, and counted as a function of time. The characteristics of the VUV undulator radiation used for product photoionization have also been previously described.[20] The time-of-flight mass spectra of each individual positive ion were recorded with the excimer laser fluence ranging from 60 to 1400 mJ/cm^2 for power-dependent measurements. In some cases, the VUV radiation was tuned to check the crackdown pattern of the ions of interest.

Additional spectroscopic experiments were performed at Brookhaven National Laboratory to compare the yields of CHBr following $CHBr_3$ excitation at 193 and 248 nm. The spectrometer uses frequency modulated (FM) transient absorption of a cw Ti:sapphire laser and a multipass Herriott cell with a slowly flowing mixture of $CHBr_3$ and He. The technique[21] and apparatus[16] have been previously described.

The $CHBr_3$ (99%) was obtained from a commercial source and was used without further purification.

III. Results and Analysis

A. Photofragment Translational Spectroscopy Experiments. There are several photodissociation pathways that are energetically accessible in the UV region (eqs 1−5).[4,6,22] Only

$$CHBr_3 \rightarrow CHBr_2 + Br \qquad \Delta_r H^0 = 63.8 \text{ kcal/mol} \quad (1)$$

$$CHBr_3 \rightarrow CHBr + Br_2 \qquad \Delta_r H^0 = 83.3 \text{ kcal/mol} \quad (2)$$

$$CHBr_3 \rightarrow CBr_2 + HBr \qquad \Delta_r H^0 = 59.0 \text{ kcal/mol} \quad (3)$$

$$CHBr_3 \rightarrow CHBr + 2Br \qquad \Delta_r H^0 = 129.0 \text{ kcal/mol} \quad (4)$$

$$CHBr_3 \rightarrow CBr + Br + HBr \qquad \Delta_r H^0 = 126.0 \text{ kcal/mol} \quad (5)$$

channels 1−3 are allowed via single-photon absorption at 248 nm. Time-of-flight (TOF) mass spectra of Br (*m*/*z* 79, 81), HBr (*m*/*z* 80, 82), CBr (*m*/*z* 93), CHBr (*m*/*z* 94), CBr_2 (*m*/*z* 172), and $CHBr_2$ (*m*/*z* 173) were collected. Center-of-mass translational energy distributions, $P(E_T)$, were obtained from the time-of-flight (TOF) spectra using the forward convolution (FC) technique.[23] The forward convolution fitting of secondary photodissociation processes has been discussed in detail previously.[24] A primary $P(E_T)$ distribution is first chosen to represent the translational energy of those primary fragments that undergo secondary photodissociation.[25] All spectra were recorded using unpolarized light at 248 nm. For all the TOF spectra presented, circles represent the data and lines represent forward convolution fits.

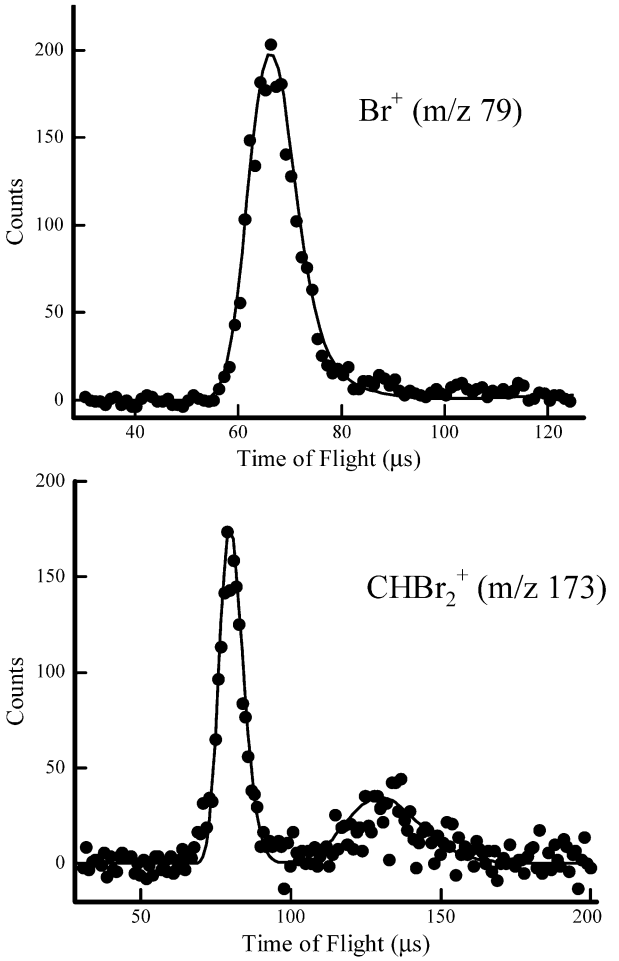

Figure 1. TOF spectra of Br^+ (*m*/*z* 79) and $CHBr_2^+$ (*m*/*z* 173) at 10° obtained at low laser fluence to minimize the contribution from multiphoton processes.

The TOF spectra of Br^+ (*m*/*z* 79) and $CHBr_2^+$ (*m*/*z* 173) shown in Figure 1 were taken at a laboratory angle of 10° and ionization energies of 13.8 and 12 eV, respectively. The Br atoms arise from either single-photon dissociation (reaction 1) or multiphoton dissociation channels (reactions 4 and 5). To minimize the contribution from multiphoton dissociation, the Br (*m*/*z* 79) spectra were taken with low laser fluence of 60 mJ/cm^2. The low laser fluence Br and $CHBr_2$ spectra (Figure 1) can be fitted using a single center-of-mass $P(E_T)$ distribution, shown in Figure 2. The two peaks evident in the $CHBr_2$ TOF spectrum represent fragments scattered forward and backward with respect to the molecular beam velocity. The fits indicate that at low laser fluence, Br atoms are primarily produced from C−Br bond cleavage. The Br TOF spectra did not show any significant differences using VUV ionization photon energies from 12.0 to 15.8 eV, suggesting a minimal contribution from dissociative ionization of other photofragments. The $P(E_T)$ distribution of the $CHBr_2 + Br$ channel is nearly Gaussian in

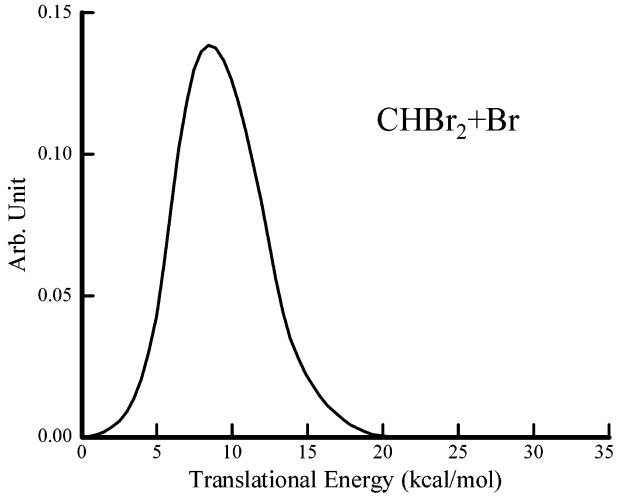

Figure 2. $P(E_T)$ distribution of $CHBr_2$ + Br channel derived from fitting the TOF spectra in Figure 1.

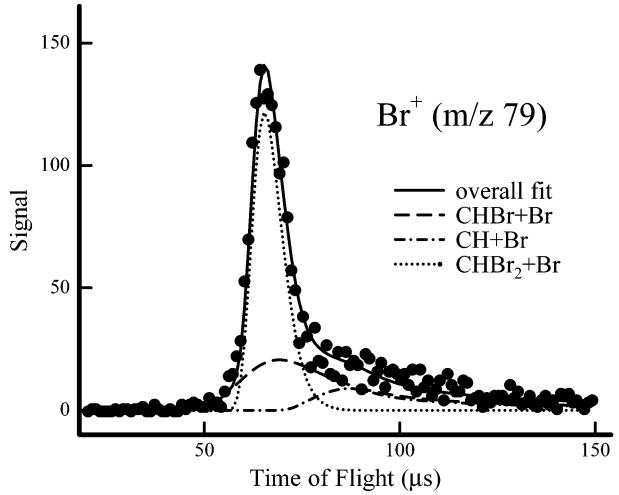

Figure 3. TOF spectrum of Br^+ (m/z 79) taken with higher laser fluence (1400 mJ/cm^2). The forward convolution fitting is improved by including the contributions from the photodissociation of $CHBr_2$ and CHBr. The dotted line represents dissociative ionization of $CHBr_2$, the dashed line represents the photodissociation of $CHBr_2$, and the dot−dash line represents the photodissociation of CHBr.

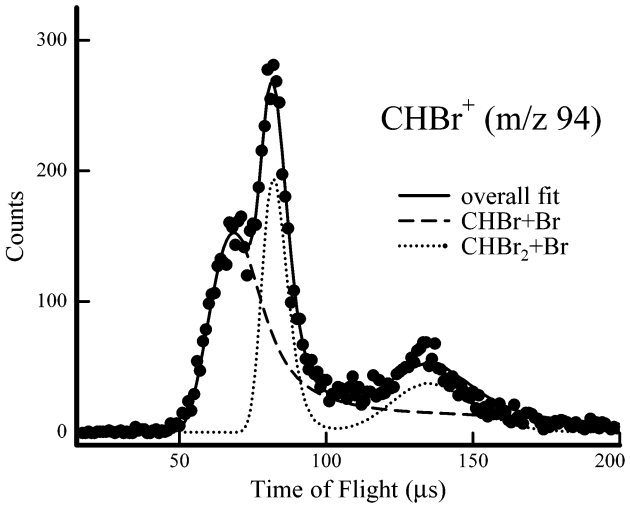

Figure 4. TOF spectrum of $CHBr^+$ (m/z 94) at a laboratory angle of 10° with ionization energy of 10 eV. The contributions from the different dissociation channels are indicated.

shape with a maximum at 8.4 kcal/mol and a fwhm of 6.7 kcal/mol. The soft fragment impulsive model usually provides a reasonable estimation of the fraction of the available energy that is partitioned into translational energy for dissociation occurring on a repulsive potential energy surface.[26,27] According to this model, 0.19 of the total available energy will be partitioned into translation for the $CHBr_2$ + Br channel. At 248 nm, the total available energy is 51.4 kcal/mol with a C−Br bond energy of 63.8 kcal/mol according to ab initio calculations by McGivern et al.[6] Assuming that the Br atoms are formed in their electronic ground state ($^2P_{3/2}$) the impulsive model predicts an average translational energy of 9.8 kcal/mol. Because the spin−orbit splitting between the ground and excited state in the Br atom is 10.6 kcal/mol,[28] the total available energy will decrease to 40.8 kcal/mol if the Br atom is at its excited state, lowering the average translational energy to 7.8 kcal/mol. Both states of Br have been observed by Xu et al. for bromoform dissociation at 234 and 267 nm and a 2.3 branching ratio for $Br(^2P_{3/2})$:$Br(^2P_{1/2})$ products at 267 nm was reported.[8] It is reasonable, therefore, to assume that both ground- and excited-state Br atoms are produced at 248 nm and our measured translational energy represents a weighted average of these two channels.

The $CHBr_2$ TOF spectra show a linear power dependence at the lower laser fluences but exhibit saturation behavior at higher fluences. This behavior is expected over our range of laser fluences on the basis of the reported cross section of bromoform at 248 nm of 1.9×10^{-18} cm^2.[4] The power dependence of the Br TOF spectra was determined using laser fluences up to 1400 mJ/cm^2. A broad feature at longer flight times appears with increasing laser power, as shown in Figure 3. This signal initially exhibits a quadratic dependence on laser fluence that decreases to less than quadratic at the highest fluences employed. No momentum-matched counterpart to the slow feature in the Br TOF can be observed in the $CHBr_2$ TOF spectra using the same laser fluence. The secondary photodissociation of both $CHBr_2$ and CHBr can produce Br atoms (channels 6 and 7, respectively). The dissociation of CHBr has been previously suggested

$$CHBr_2 \rightarrow CHBr + Br \qquad \Delta_r H^0 = 65.2 \text{ kcal/mol} \qquad (6)$$

$$CHBr \rightarrow CH + Br \qquad \Delta_r H^0 = 79.5 \text{ kcal/mol} \qquad (7)$$

as the source of CH(A,B) radicals using $CHBr_3$ as precursor.[14,15] We have assigned the additional features in the high-power Br atom TOF spectra to channels 6 and 7.

Evidence for channel 6, the secondary photodissociation of $CHBr_2$, is observed in the CHBr TOF spectrum shown in Figure 4. The spectrum was taken at a laboratory angle of 10° with an ionization energy of 10 eV. The solid line represents the overall forward convolution fit, the dotted line represents the fits to the dissociative ionization of $CHBr_2$, and the dashed line represents the secondary photodissociation of $CHBr_2$ (elimination of Br). The dashed line is momentum matched to the corresponding dashed line contribution in the high-fluence Br TOF spectra (Figure 3). The TOF spectra of CHBr taken at two different laser fluences are shown in Figure 5. Bilogarithmic plots show that the $CHBr^+$ signal arising from dissociative ionization has a slope of 0.9 ± 0.1 whereas the $CHBr_2$ secondary photodissociation signal has a slope of 1.8 ± 0.1 at fluences below 200 mJ/cm^2. The $P(E_T)$ distribution for the CHBr + Br channel shown in Figure 6 peaks at 10 kcal/mol with an average energy of 15 kcal/mol. The soft-fragment impulsive model predicts that almost one-fourth of the available energy will be

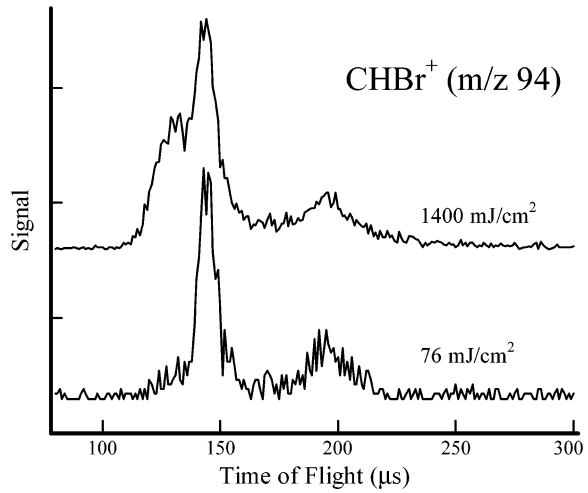

Figure 5. $CHBr^+$ (*m*/*z* 94) TOF spectra taken with two different laser fluences. The relative intensities of the features assigned to the multiphoton dissociation channels increase compared to the signal attributed to the single-photon channel.

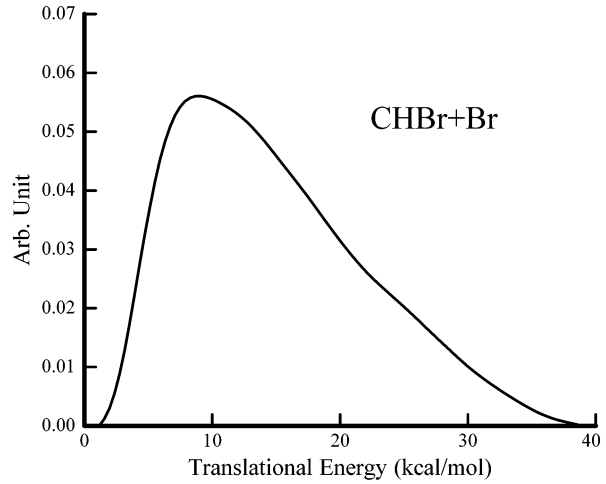

Figure 6. $P(E_T)$ distribution for the CHBr + Br channel of secondary photodissociation of $CHBr_2$ derived from fitting the high-fluence TOF spectra in Figures 3 and 4.

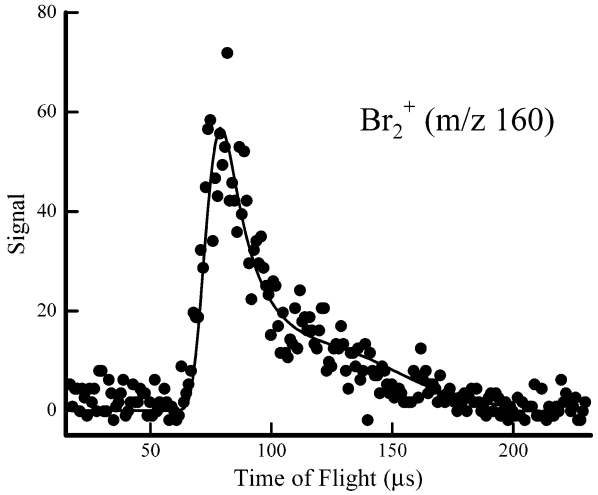

Figure 7. Br_2^+ (*m*/*z* 160) TOF spectrum taken at a laboratory angle of 10° with ionization energy of 12 eV. The signal is fitted with a single $P(E_T)$ distribution shown in Figure 8.

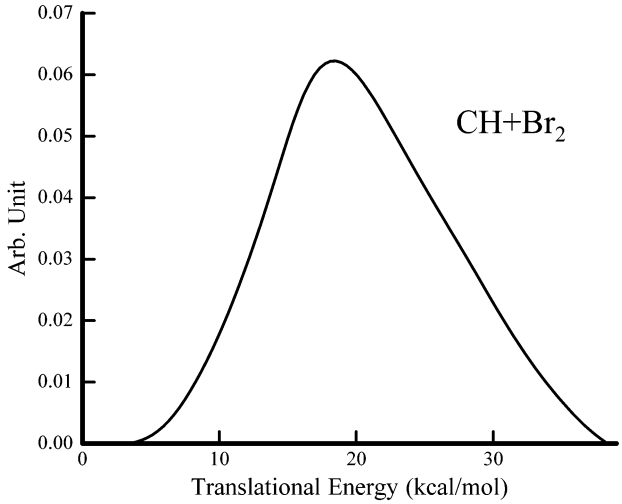

Figure 8. $P(E_T)$ distribution for the molecular bromine elimination channel from bromoform.

partitioned into translational energy for this channel. Based on the average translational energy for the $CHBr_2$ + Br channel, the average available energy for CHBr and Br fragments will be 80−90 kcal/mol assuming electronic ground-state CHBr and Br as products. Therefore, the measured $P(E_T)$ distribution for the secondary photodissociation of $CHBr_2$ appears consistent with the impulsive model prediction.

No additional components are required to fit the $CHBr^+$ TOF spectra, suggesting that the elimination of Br_2 from $CHBr_3$ is a minor channel. Molecular bromine photofragments are observed, however. The Br_2 TOF spectrum shown in Figure 7 was taken at a laboratory angle of 10° with an ionization energy of 12 eV. The signal exhibits a quadratic (1.9 ± 0.1) dependence on the laser fluence, indicating that the dissociation results from a multiphoton process. We attribute the observed Br_2 to the photodissociation of $CHBr_2$ radicals,

$$CHBr_2 \rightarrow CH + Br_2 \qquad \Delta_r H^0 = 99.4 \text{ kcal/mol} \qquad (8)$$

The $P(E_T)$ distribution used to fit the CH + Br_2 channel is shown in Figure 8. The distribution is nearly symmetric in shape and peaks at 18 kcal/mol with a fwhm of 15 kcal/mol. No effort was made to collect CH^+ (*m*/*e* 13) TOF spectra because the original intention of our study was the elucidation of the single-photon channels and CH can only arise from multiphoton dissociation. Forward convolution fitting of the CH^+ could, however, provide constraints on both the CH + Br and CH + Br_2 channels.

The ionization energy dependence of the $CHBr^+$ TOF spectra, taken with 10 and 12 eV ionization energies, is shown in Figure 9. The ionization potentials are 8.9 and 8.3 eV for CHBr and $CHBr_2$, respectively.[29,30] The dissociative ionization of $CHBr_2$ requires 65.2 kcal/mol more energy than the ionization of CHBr. Decreasing the ionization energy from 12 to 10 eV decreases the signal attributed to the dissociative ionization of $CHBr_2$ relative to the signal attributed to the CHBr fragments providing confirmation of our assignments of the components observed in the $CHBr^+$ TOF spectra.

The elimination of HBr from $CHBr_3$ is also accessible following single-photon absorption. We find, however, that although the HBr elimination is the most energetically favorable channel, the observed HBr signal cannot be attributed to a single-photon process according to our power dependence measurements. The CBr_2 (*m*/*z* 172) TOF spectrum shown in Figure 10, taken at a laboratory angle of 10° and an ionization energy of 12 eV, consists only of signal from the dissociative ionization

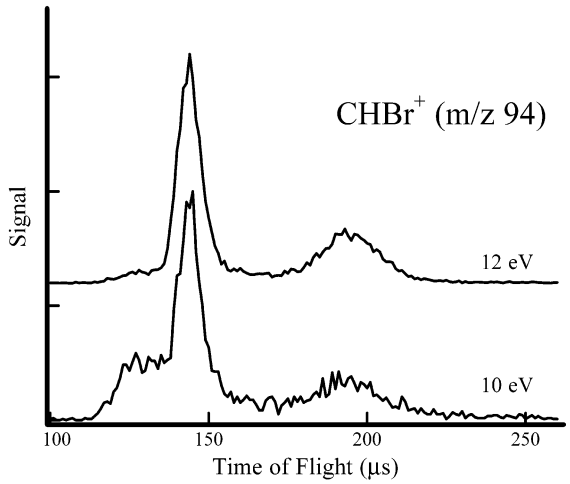

Figure 9. $CHBr^+$ (*m*/*z* 94) TOF spectrum taken with two different ionization energies.

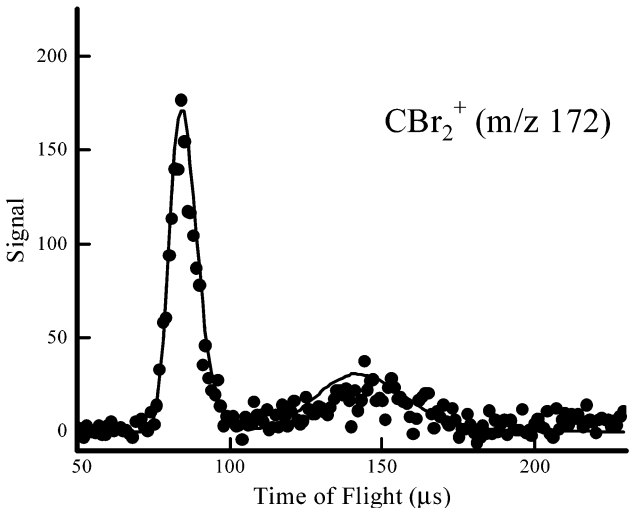

Figure 10. TOF spectrum of CBr_2^+ (*m*/*z* 172). The CBr_2 signal arises solely from the dissociative ionization of $CHBr_2$.

of $CHBr_2$ (channel 1). The power dependence of CBr_2 signal is linear. On the basis of these observations we believe that the single-photon elimination of HBr from $CHBr_3$ is negligible at 248 nm.

The HBr (*m*/*z* 82) TOF spectrum shown in the upper panel of Figure 11 was taken at a laboratory angle of 10° and an ionization energy of 15 eV. There is a small contribution from the dissociative ionization of $CHBr_2$ represented by the dash−dot line. The majority of HBr observed is attributed to the secondary photodissociation of $CHBr_2$ represented by the dashed line. The CBr (*m*/*z* 91) TOF spectrum shown in the lower panel was taken at a laboratory angle of 10° and an ionization energy of 13 eV. Two components are observed in CBr TOF spectrum, the dissociative ionization of $CHBr_2$ represented by the dash−dot line and the secondary photodissociation of $CHBr_2$ represented by the dashed line. The secondary photodissociation of $CHBr_2$ to give CBr + HBr fragments has a $P(E_T)$ distribution shown in Figure 12. The $P(E_T)$ distribution is slightly asymmetric, which peaks at 9 kcal/mol with a fwhm of 10 kcal/mol. The signal associated with this channel in both TOF spectra exhibited a quadratic power dependence on the laser fluence that started to show saturation behavior at the highest fluences employed.

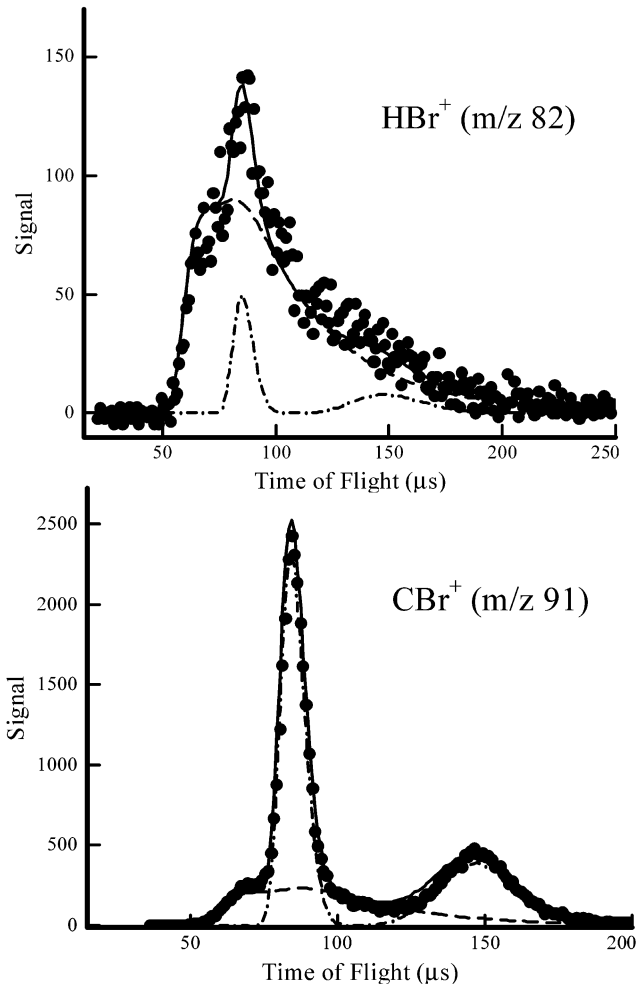

Figure 11. (Upper) TOF spectrum of HBr^+ (*m*/*z* 82). The dash−dot line represents the dissociative ionization of $CHBr_2$, and the dashed lines represent the CBr + HBr channel from the secondary photodissociation of $CHBr_2$. (Lower) TOF spectrum of CBr^+ (*m*/*z* 91). The dash−dot line represents the dissociative ionization of $CHBr_2$, and the dashed line represent the CBr + HBr channel from the secondary photodissociation of $CHBr_2$.

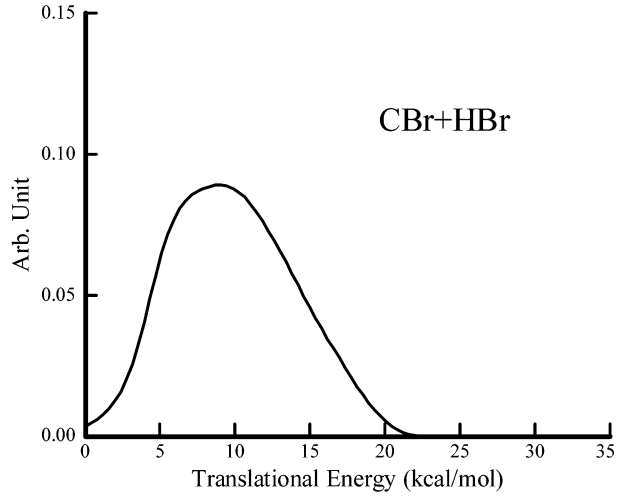

Figure 12. $P(E_T)$ distribution for the CBr + HBr channel from the secondary photodissociation of $CHBr_2$.

B. Laser Absorption Spectroscopy of CHBr. Independent laser absorption experiments were undertaken to test for the possibility of a single photon channel producing Br_2 and CHBr in the 248 nm photodissociation of bromoform. The frequency

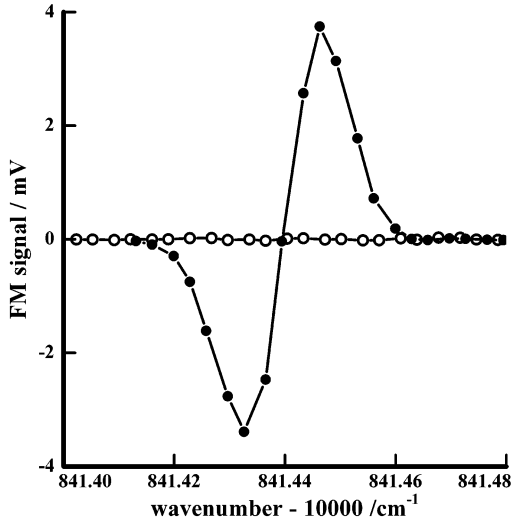

Figure 13. Comparison of peak spectral intensities for a CHBr line following photodissociation of $CHBr_3$ at 193 (filled circles) and 248 nm (open circles). The derivative line shape is measured by frequency modulation absorption spectroscopy and illustrates at least a 200:1 reduction in the signal level as the photolysis wavelength is changed from 193 to 248 nm.

modulated transient absorption spectrometer at Brookhaven National Laboratory has been previously used to measure CHBr spectroscopy and kinetics, following 193 nm photodissociation of bromoform.[16] A direct comparison of CHBr signal strength using 193 and 248 nm excimer laser photolysis permits an assessment of the relative yields of CHBr at these wavelengths. We further intended to measure the power dependence of the CHBr signal at 248 nm to characterize any multiphoton pathways to CHBr.

At 193 nm, previous studies have shown CHBr to be formed with a yield of about 0.3, following spontaneous fragmentation of the single-photon, primary $CHBr_2$ photoproduct. In a flowing sample consisting of about 100 mTorr $CHBr_3$ in 1.5 Torr He, the transient absorption spectra of CHBr following 193 nm photolysis rise to a maximum in about 5 μs and decay in tens of microseconds, reflecting thermalization and reaction time scales. The strong line in Figure 13 (closed circles) is the Q(10) line in the $A(0,0,0)-X(0,1,0)$ band of CHBr, near 10 841 cm^{-1}, measured at the time of maximum absorption. Similar time-dependent signals have been observed for rotational lines of the origin band, probing the ground vibrational state of CHBr.[18] The 193 nm laser fluence was 30 mJ/cm^2 for this measurement, and the plotted spectrum reflects the peak intensity, observed 4−6 μs following the ArF excimer laser pulse.

Changing the excimer laser gas from ArF to the KrF mixture, exchanging one dichroic beam steering mirror, and repeating the scan on the same flowing mixture resulted in the null spectrum displayed in Figure 13 (open circles). At no time during the 100 μs observation time was any absorption signal observed in this spectral region, putting a small upper bound on the relative yield of CHBr production at 248 nm relative to that at 193 nm. Despite the absence of CHBr absorption signals, visibly stronger violet emission from excited CH was observed with 248 nm than with 193 nm. The 248 nm fluence exceeded the 193 nm fluence by a factor of 1.8 in the displayed scans, with all else remaining constant. On the basis of the noise level of these measurements, we set an upper bound of 1:200 for the relative populations of the detected rovibrational level produced at 248 nm relative to the 193 nm reference. The absorption cross section of $CHBr_3$ at 248 nm is smaller than that at 193 nm by a factor of 1.8, the same factor by which the 248 nm laser fluence exceeded the 193 nm fluence. If a single photon process produced Br_2 + CHBr at 248 nm with a quantum yield as large as 0.2, we should expect CHBr signals of comparable intensities in these two scans. We conclude the single-photon yield of Br_2 + CHBr at 248 nm is at least a factor of 100 smaller. In addition, we were unable to detect any CHBr that we could attribute to multiphoton pathways at 248 nm.

Additional related experiments at 266 nm did produce easily detectable CHBr signals at lower fluences. The growth of low-energy CHBr rovibronic states is slower than at 193 nm, as previously reported.[18] This is consistent with a requirement for more extensive relaxation from a higher energy initial distribution of CHBr formed by more than one 266 nm photon. The pressure, power, and time-dependent CHBr signals we observed from $CHBr_3$ at 266 nm were complex and will require further study to confirm and interpret. We suspect the striking differences between 248 and 266 nm experiments are attributable to differences in the *secondary* photochemistry of $CHBr_2$. The branching among Br_2 + CH, HBr + CBr, and Br + HCBr dissociation channels may change abruptly with excitation energy, or the absorption cross section of $HCBr_2$ may be changing rapidly in this region.

IV. Discussion

A. Br_2 Elimination Channel. Our measurements indicate that the formation of Br_2 requires at least two 248 nm photons and involves the secondary photodissociation of $CHBr_2$. It is difficult to determine the relative yields of Br_2, HBr, and Br from photodissociation of $CHBr_2$ because the internal energy of the fragments, and hence photoionization cross sections, may differ substantially. We postulate that the majority of CHBr products observed in the current experiment very likely in the experiments of Liu et al. arise from sequential photodissociation of $CHBr_3$ and not from the primary CHBr + Br_2 channel. The elimination of Br_2 from the photodissociation of $CHBr_2$ can only result in ground-state CH on the basis of energetics. This mechanism is consistent with recent measurements measuring a quadratic power dependence of the formation of $CH(X\ ^2\Pi)$ at 248 nm.[12,13] Previous studies reporting evidence of a three-photon mechanism to produce excited-state CH, detected via $CH(A^2\Delta \rightarrow X^2\Pi)$ emission, likely characterized the sequential loss of three Br atoms.[14,15]

B. HBr Elimination from $CHBr_2$. There is a significant difference between the $P(E_T)$ distributions for the CBr + HBr at 248 nm in the current study and the distribution measured at 193 nm (ref 6), which peaked near zero translational energy. This is not surprising given the dissimilar formation mechanisms. The $P(E_T)$ distribution for the $CHBr_2 \rightarrow$ HBr + CBr channel at 193 nm peaks is consistent with a spontaneous decomposition mechanism. Theoretical calculations reveal that the exit channel barrier is only 0.6 kcal/mol higher than the asymptotic product energy for the HBr elimination, resulting in a translational energy release well described by statistical models of energy partitioning. The secondary dissociation of $CHBr_2$ at 248 nm, however, requires an additional photon and the translational energy suggests dissociation on a repulsive potential.

CASSCF and MRCI calculations of CH_2Br by Li et al. reveal that the low-lying excited states are all repulsive along the C−Br bond, indicating the C−Br bond fission is the dominant photodissociation channel in the UV region.[31] There is evidence for more complicated dynamics in the transient resonance Raman spectra $CHBr_2$ radical in methanol solution.[32,33] The

Raman spectra show activity not only in the C−Br stretch but also in the Br−C−Br bend and combinations of these modes, suggesting a more multidimensional photodissociation than CH_2-Br, which exhibits only a C−Br stretching progression. These studies provide indirect support for molecular elimination channels in addition to the CHBr + Br channel in the photodissociation of $CHBr_2$.

C. Br Atom Quantum Yield. The photodissociation quantum yields of $CHBr_3$ have been reported recently by several groups in the wavelength region from 193 to 324 nm.[6,7,8] The experiments by Bayes and co-workers represent absolute quantum yield measurements, and the authors conclude that the Br atom quantum yields at wavelengths >300 nm should be unity.[7] Although the quantum yields reported in this wavelength region were less than unity, the authors attributed this finding to random errors related to the small absorption cross sections and weak signals at long wavelengths. At 266 nm Bayes et al. report a Br quantum yield of 0.76 ± 0.03, which was interpreted to indicate the involvement of other dissociation channels. Xu et al. subsequently observed Br_2 formation from $CHBr_3$ photodissociation at 266 and 235 nm.[8] Their reported Br_2 quantum yields of 0.16 and 0.26 suggested that Br_2 elimination was the reason that the Br atom quantum yields were less than unity. The authors used the CHBr and $CHBr_2$ signal intensities to estimate the branching ratio between the C−Br bond fission and Br_2 elimination channels by assuming the photoionization cross sections of CHBr and $CHBr_2$ at 118 nm were equivalent. Verification of this assumption requires more experimental evidence because it may significantly alter the branching ratio derived by Xu et al. The fragment channels were also not momentum matched, suggesting that the fragments may derive from different processes. Finally, no test for linearity of fragment yields with laser power was performed.

Theoretical calculations[5] suggest that the dominant primary photodissociation channel of bromoform in the UV region is prompt C−Br bond fission, which would result in a primary Br quantum yield of unity. Although the PTS experiments by McGivern et al. at 193 nm (ref 6) and the current study are not well suited for determining absolute quantum yields, they can often provide accurate relative quantum yields. We find that at 248 nm, as is the case at 193 nm, the only single-photon dissociation pathway is the $CHBr_2$ + Br channel. Unless there are nondissociative pathways that participate at 248 nm, which we consider unlikely given the prompt fragmentation channel, the Br atom quantum yield should be considered to be unity at this wavelength. It is difficult to reconcile this conclusion with previous reports at 266 and 235 nm, although it is possible that several excited states may be involved in the dissociation, which lead to different products over this narrow wavelength range. Though we observe Br_2 fragments, our experiments demonstrate that these fragments arise from multiphoton dissociation. Transient absorption spectroscopy of CHBr confirms that a single-photon CHBr + Br_2 channel is minor. Because the Br quantum yields and branching ratios between different dissociation channels are important for atmospheric chemistry modeling, more experimental and theoretical studies will be needed for resolution of the contradictory results. To this end, additional PTS experiments performed at 266 nm may prove extremely insightful.

Acknowledgment. We thank Dr. K. Bayes, Dr. W. S. McGivern, Dr. J. S. Francisco, and Dr. S. P. Sander for their valuable comments. We also thank Dr. B.-C. Chen for help with the CHBr experiments. The experiments were conducted at the Advanced Light Source, Lawrence Berkeley National Laboratory, which is supported by the Director, Office of Energy Research, Office of Basic Energy Science, Chemical Sciences Division of the U.S. Department of Energy under contract No. DE-AC03-76SF00098. Support for this project was provided by the Texas Research Endowment Program, a Research Enhancement Grant from Texas A&M University, and the Robert A. Welch Foundation (Grant Number A-1405). The work at Brookhaven National Laboratory was performed under Contract No. DE-AC02-98CH10886 with the U.S. Department of Energy and supported by its Division of Chemical Sciences.

References and Notes

(1) Molina, M. J.; Rowland, F. S. *Nature* **1974**, *248*, 810.

(2) Solomon, S.; Mills, M.; Heidt, L. E.; Pollock, W. H.; Tuck, A. F. *J. Geophys. Res.* **1992**, *97*, 25.

(3) Garcia, R. R.; Solomon, S. *J. Geophys. Res.* **1994**, *99*, 12937.

(4) DeMore, W. B.; Sander, S. P.; Golden, D. M.; Hampson, R. F.; Kurylo, M. J.; Howard, C. J.; Ravishankara, A. R.; Kolb, C. E.; Molina, M. J. Chemical Kinetics and Photochemical Data for Use in Stratospheric Modeling. Evaluation Number 11. NASA JPL Publ. No. 94-26; NASA: Washington, DC, 1994.

(5) Peterson, K. A.; Francisco, J. S. *J. Chem. Phys.* **2002**, *117*, 6103.

(6) McGivern, W. S.; Sorkhabi, O.; Suits, A. G.; Derecskei-Kovacs, A.; North, S. W. *J. Phys. Chem. A* **2000**, *104*, 10085.

(7) Bayes, K. D.; Toohey, D. W.; Friedl, R. R.; Sander, S. P. *J. Geophys. Res.* **2003**, *108*, 4095.

(8) Xu, D.; Francisco, J. S.; Huang, J.; Jackson, W. M. *J. Chem. Phys.* **2002**, *117*, 2578.

(9) Butler, J. E.; Fleming J. W.; Goss, L. P.; Lin, M. C. *Chem. Phys.* **1981**, *56*, 355.

(10) Fulle, D.; Hippler, H. *J. Chem. Phys.* **1996**, *105*, 5423.

(11) Wang, C.-C.; Chen, Y.-P.; Chin, T.-L., Huang, H.-Y.; Lin, K.-C. *J. Chem. Phys.* **2000**, *112*, 10204.

(12) Kind, M.; Stuhl, F.; Tzeng, Y.-R.; Alexander, M. H.; Dagdigian, P. J. *J. Chem. Phys.* **2001**, *114*, 4479.

(13) Vaghjiani, G. L. *J. Chem. Phys.* **2003**, *119*, 5388.

(14) Lichtin, D. A.; Berman, M. R.; Lin, M. C. *Chem. Phys. Lett.* **1984**, *108*, 18.

(15) Lindner, J.; Ermisch, K.; Wilhelm, R. *Chem. Phys.* **1998**, *238*, 329.

(16) Chang, B.-C.; Sears, T. J. *J. Chem. Phys.* **1996**, *105*, 2135.

(17) Marr, A. J.; North, S. W.; Sears, T. J.; Ruslen, L.; Field R. W. *J. Mol. Spectrosc.* **1998**, *188*, 68.

(18) Liu, W. L.; Chang, B. C. *J. Chin. Chem. Soc.-Taip.* **2001**, *48*, 613.

(19) Yang, X.; Blank, D. A.; Lin, J.; Heimann, P. A.; Wodtke, A. M.; Suits, A.; Lee, Y. T. *Rev. Sci. Instrum.* **1997**, *68*, 3317.

(20) Koike, M.; Heimann, P. A.; Kung, A. H.; Namioka, T.; DiGennaro, R.; Gee, B.; Yu, N. *Nucl. Instrum. Methods Phys. Res.* **1994**, *347*, 282. Heimann, P. A.; Koike, M.; Hsu, C. W.; Evans, M.; Ng, C. Y.; Blank, D.; Yang, X. M.; Flaim, C.; Suits, A. G.; Lee, Y. T. *SPIE Proc.* **1996**, p 2865.

(21) Hall, G. E.; North, S. W. *Annu. Rev. Phys. Chem.* **2000**, *51*, 243.

(22) Atkinson, R.; Baulch, D. L.; Cox, R. A.; Hampson, R. F.; Kerr, J. A.; Rossi, J.; Troe, J. Evaluated Kinetic and Photochemical Data for Atmopheric Chemistry: Supplement VIII, Halogen Species Evaluation for Atmospheric Chemistry. *J. Phys. Chem. Ref. Data* **2000**, *29*, 167.

(23) A. M. Wodtke, Ph.D. Thesis, University of California, Berkeley, 1986. X. Zhao, Ph.D. Thesis, University of California, Berkeley 1989.

(24) Zhao, X.; Nathanson, G. M.; Lee, Y. T. *Acta Physico-Chim. Sinica* **1992**, *8*, 70.

(25) We have assumed that the primary translational energy distribution derived from fitting the $CHBr_2$ TOF spectra represents the translational energy distribution of the $CHBr_2$ fragments that undergo secondary photodissociation. This is tantamount to assuming the absorption cross section is independent of $CHBr_2$ internal energy.

(26) Busch, G. E.; Wilson, K. R. *J. Chem. Phys.* **1972**, *56*, 3639.

(27) Tuck, A. F. *J. Chem. Soc., Faraday Trans.* **1977**, *73*, 689.

(28) Tech, J. L. *J. Res. Nat. Bur. Stand.* **1963**, *67A*, 505.

(29) Li, Z.; Francisco, J. S. *J. Chem. Phys.* **1998**, *109*, 134.

(30) Andrews, L.; Dyke, J. M.; Jonathan, N.; Keddar, N.; Morris, A. *J. Phys. Chem.* **1984**, *88*, 1950.

(31) Li, Y.; Francisco, J. S. *J. Chem. Phys.* **2001**, *114*, 2879.

(32) Li, Y.-L.; Zuo, P.; Phillips, D. L. *Chem. Phys. Lett.* **2002**, *364*, 573.

(33) Li, Y.-L.; Leung, He; Phillips, D. L. *Mol. Phys.* **2002**, *100*, 2659.